Arch Toxicol (2014) 88:145–160
DOI 10.1007/s00204-013-1084-7

GENOTOXICITY AND CARCINOGENICITY

A novel genotoxicity assay of carbon nanotubes using functional macrophage receptor with collagenous structure (MARCO)-expressing chicken B lymphocytes

Mohiuddin · Islam Shamima Keka · Terry John Evans · Kouji Hirota · Hiroyasu Shimizu · Koichi Kono · Shunichi Takeda · Seishiro Hirano

Received: 22 March 2013 / Accepted: 20 June 2013 / Published online: 21 August 2013

Abstract Although carbon nanotubes (CNTs) are promising nanomaterials, their potential carcinogenicity is a major concern. We previously established a genetic method of analyzing genotoxicity of chemical compounds, where we evaluated their cytotoxic effect on the DT40 lymphoid cell line comparing DNA-repair-deficient isogenic clones with parental wild-type cells. However, application of our DT40 system for the cytotoxic and genotoxic evaluation of nanomaterials seemed to be difficult, because DT40 cells only poorly internalized nanoparticles. To solve this problem, we have constructed a chimeric gene encoding a trans-membrane receptor consisting of the 5′ region of the transferrin receptor (TR) gene (to facilitate internalization of nanoparticles) and the 3′ region of the macrophage receptor with collagenous structure (MARCO) gene (which is a receptor for environmental particles). We expressed the resulting MARCO-TR chimeric receptor on DNA-repair-proficient wild-type cells and mutants deficient in base excision repair (*FEN1*$^{-/-}$) and translesion DNA synthesis (*REV3*$^{-/-}$). We demonstrated that the chimera mediates uptake of particles such as fluorescence-tagged polystyrene particles and multi-walled carbon nanotubes (MWCNTs), with very poor uptake of those particles by DT40 cells not expressing the chimera. MWCNTs were cytotoxic and this effect was greater in *FEN1*$^{-/-}$and *REV3*$^{-/-}$ cells than in wild-type cells. Furthermore, MWCNTs induced greater oxidative damage (measured as 8-OH-dG formation) and a larger number of mitotic chromosomal aberrations in repair-deficient cells compared to repair-proficient cells. Taken together, our novel assay system using the chimeric receptor-expressing DT40 cells provides a sensitive method to screen for genotoxicity of CNTs and possibly other nanomaterials.

Keywords Carbon nanotube · Genotoxicity · MARCO · Nanoparticles · Oxidative stress

Electronic supplementary material The online version of this article (doi:10.1007/s00204-013-1084-7) contains supplementary material, which is available to authorized users.

Mohiuddin · I. S. Keka · T. J. Evans · K. Hirota · S. Takeda (✉)
Department of Radiation Genetics, Graduate School of Medicine, Kyoto University, Kyoto 606-8501, Japan
e-mail: stakeda@rg.med.kyoto-u.ac.jp

Mohiuddin · H. Shimizu · K. Kono
Department of Hygiene and Public Health, Graduate School of Medicine, Osaka Medical College, Osaka 569-8686, Japan

Present Address:
K. Hirota
Department of Chemistry, Tokyo Metropolitan University, 1-1 Minami-Ohsawa, Hachioji, Tokyo 192-0397, Japan

S. Hirano (✉)
Environmental Nanotoxicology Section, RCER, National Institute for Environmental Studies, Tsukuba, Ibaraki 305-8506, Japan
e-mail: seishiro@nies.go.jp

Introduction

There has been a large increase in the production of nanomaterials globally, with a corresponding increase in research into the potential toxicity associated with their use. Carbon nanotubes (CNTs) in particular have incredible potential in many applications because of their unique chemical, physical, and electronic properties. They have therefore attracted the interest of toxicologists, material scientists, and regulatory agencies—not least of all because the commercial use of CNTs may threaten health (Donaldson et al. 2006). For example, intratracheal instillation of

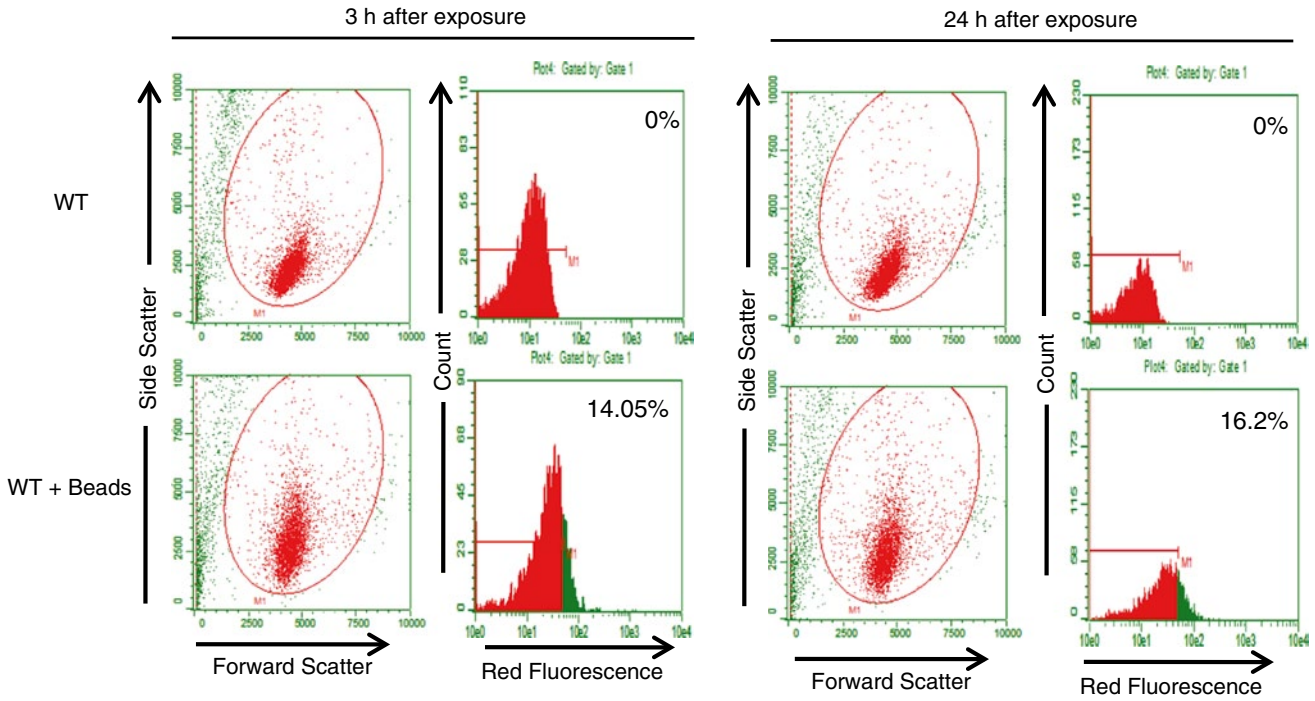

Fig. 1 Chicken DT40 cells are unable to recognize polystyrene particles efficiently. Chicken DT40 cells were exposed to 200-nm red fluorescent microspheres for 24 h. The cellular association of microspheres was evaluated by flow cytometry after incubation for 3 and 24 h with red fluorescent microspheres. Wild-type cells cannot take up particles efficiently, and the fluorescence intensity does not increase with time

SWCNTs in the lungs of mice (Lam et al. 2004; Shvedova et al. 2005) and MWCNTs (Muller et al. 2008) or SWCNTs (Warheit et al. 2004) in the lung of rats caused inflammatory and fibrotic lesions. Several previous studies showed that both MWCNTs and SWCNTs are highly cytotoxic to many cell types, including macrophages (Hirano et al. 2008; Jia et al. 2005; Kagan et al. 2006), epithelial cells (Cui et al. 2005; Hirano et al. 2010; Ye et al. 2009), mesothelial cells (Pacurari et al. 2008; Wick et al. 2007; Nagai et al. 2011), and keratinocytes (Monteiro-Riviere et al. 2005; Shvedova et al. 2003). As carcinogenicity of these promising nanomaterials is a major concern, we aimed to develop a novel bio-assay to define the cytotoxicity associated with nanoparticles by using a genetic approach, wherein data of WT cells are used as a negative control to evaluate data obtained from any gene-disrupted isogenic clones such as DNA-repair mutants.

Particles are taken up through phagocytosis, which seems to be independent of the primary size of particles. This process can be mediated by the macrophage receptor with collagenous structure (MARCO) (Kanno et al. 2007; Hirano et al. 2012). MARCO belongs to the scavenger receptor class A family of proteins, and is expressed on the cell surface of macrophages (Elomaa et al. 1998). It plays a pivotal role in innate immunity and apoptotic clearance (Greaves and Gordon 2005), and has been shown to mediate binding and ingestion of unopsonized environmental particles such as iron oxide (Fe_2O_3), titanium dioxide (TiO_2), quartz, diesel exhaust dust, and latex beads (Kobzik 1995; Palecanda et al. 1999). Furthermore, MARCO is involved in the lung's defense against pneumococcal pneumonia (Arredouani et al. 2004; Elomaa et al. 1998; van der Laan et al. 1999) and clearance of silica (SiO_2) particles from the lung (Thakur et al. 2009). The cysteine-rich scavenger receptor domain of MARCO, which is important for ligand binding, is encoded by the 3′ region of the MARCO gene (Elomaa et al. 1995). Recently, it has been proved that MARCO plays a crucial role in the uptake of polystyrene beads of a variety of sizes, including nano-sized (Kanno et al. 2007) as well as fibrous particles, specifically MWCNTs (Hirano et al. 2012). Thus, MARCO functions in the uptake of various types of particles.

Several previous studies have demonstrated the value of chicken DT40 B lymphocyte cell lines that are deficient in DNA-repair pathways as a unique tool for systematic genetic analysis of DNA repair in vertebrates. This is possible because the unusually high ratio of targeted to random integration allows disruption of genes involved in DNA repair (Buerstedde and Takeda 1991). A panel of DT40 clones deficient in various DNA-repair genes is also extremely useful for identifying genotoxic chemicals and environmental samples while simultaneously

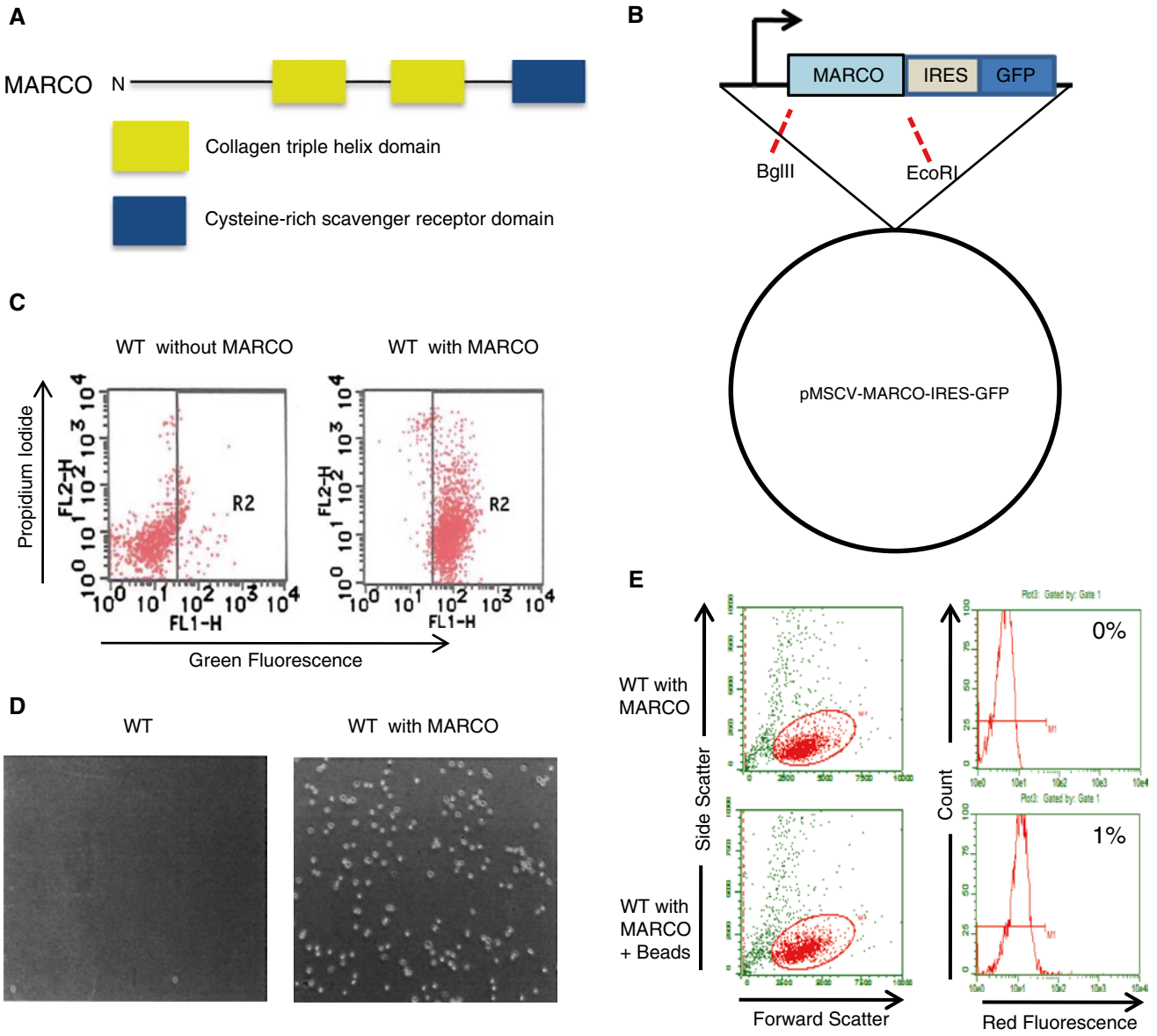

Fig. 2 Chicken DT40 cells stably expressing MARCO recognize the culture dish surface, but they are unable to recognize polystyrene particles. **a** Schematic representation of the domain structure of MARCO. **b** Schematic of the pMSCV-MARCO-IRES-GFP vector. **c** Expression levels of MARCO in WT DT40 cells analyzed by FACS. *X*-axis represents the intensity of green fluorescence (due to expression of green fluorescence protein (GFP)) and the *Y*-axis represents the propidium iodide-stained cells. **d** Chicken DT40 cells stably expressing MARCO can adhere to the bottom of the polystyrene dish. WT DT40 cells either expressing or not expressing MARCO were incubated at 0.5×10^6 cells/ml in a 24-well plate for 1 h at 39.5 °C. After removing media, each well was washed twice with PBS and the cells adhered to the culture dish were observed using microscopy (10× magnification). The MARCO-transfected cells were more adherent to the culture dish. **e** WT cells expressing MARCO were exposed to 200-nm red fluorescent microspheres for 24 h. The cellular association of microspheres was evaluated by flow cytometry. Cells expressing MARCO cannot efficiently take up particles

determining their mechanism of action (Evans et al. 2010; Ji et al. 2009, 2011a, b). Using various DNA-repair gene-disrupted clones, we can detect genotoxic agents by simply measuring cellular proliferation. This is because the vast majority of DNA damaging agents interfere with DNA replication, and thereby slow cellular proliferation more significantly in DNA-repair-deficient clones compared with DNA-repair-proficient wild-type cells. Moreover, DT40 cells have an unusually long S phase, about 70 % of the whole cell cycle, and are unable to arrest at the G_1/S checkpoint after DNA damage due to the lack of a functional p53 gene (Yamazoe et al. 2004). Thus, exogenous DNA damage has a considerably stronger impact on DNA replication on DT40 cells than on other cell lines. The resulting

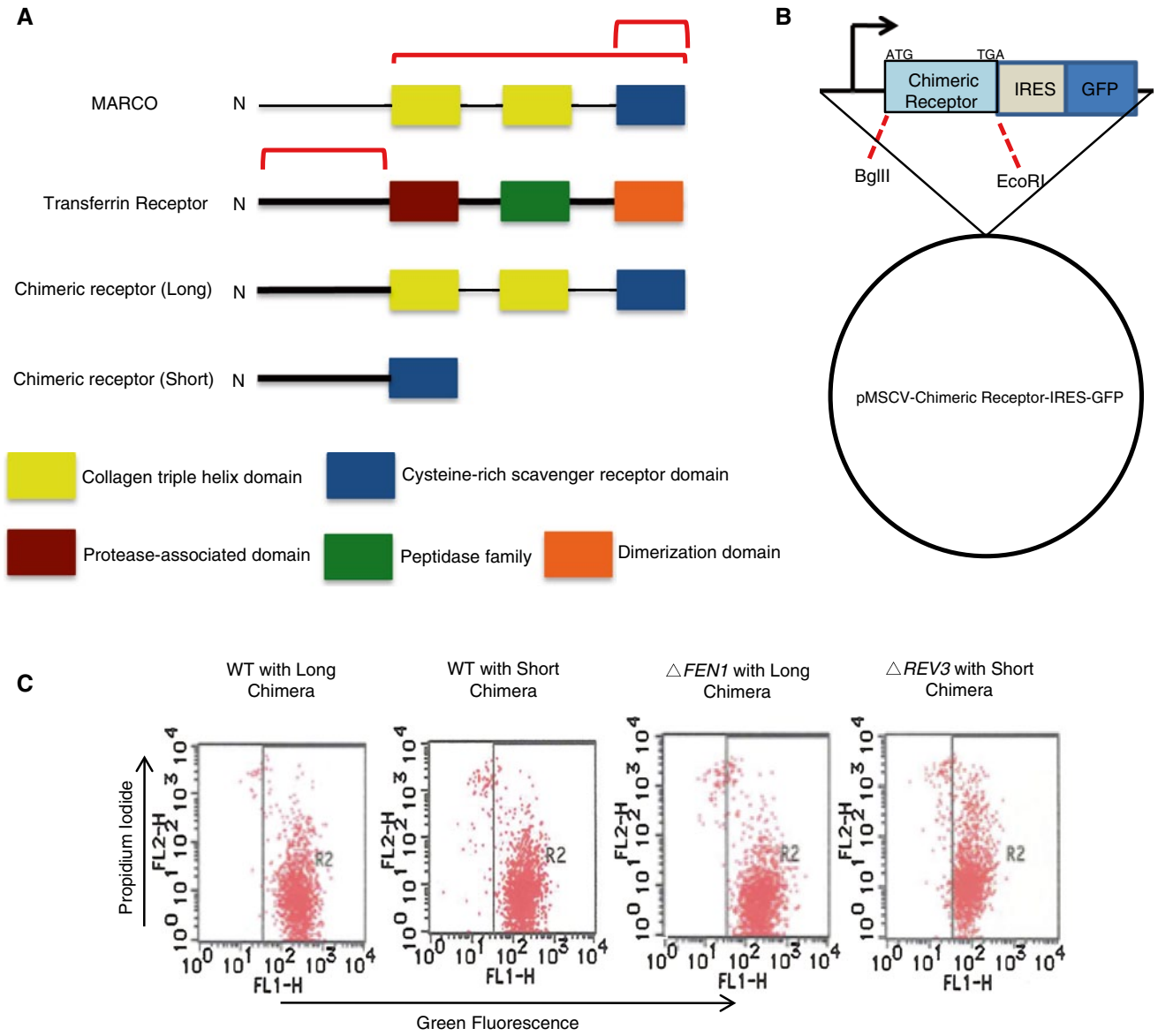

Fig. 3 Construction of functional MARCO-TR chimera-expressing DT40 strains. **a** Schematic representation of the domain structures of MARCO and transferrin receptor where the C-terminal domains of MARCO and the N-terminal region of the transferrin receptor are fused to engineer a chimeric receptor. **b** Schematic of the pMSCV-chimeric receptor-IRES-GFP vector. **c** Expression levels of MARCO-TR receptor in wild-type, *FEN1*$^{-/-}$ and *REV3*$^{-/-}$ DT40 cells analyzed by FACS. *X*-axis represents the intensity of green fluorescence and the *Y*-axis represents the propidium iodide (PI) stained cells

inhibition of DNA replication can lead to: (1) the formation of double-strand breaks (DSBs) detectable as chromosomal breaks in mitotic cells, (2) subnuclear focus formation of phosphorylated histone H2AX (γH2AX focus) detectable by an immunocytochemical method, and (3) a delay in cellular proliferation. These features of DT40 cells provide multiple advantages for research into DNA repair and their use in genotoxicity testing.

Two DNA-repair mutants were used in this study—*FEN1*$^{-/-}$ and *REV3*$^{-/-}$. Flap structure-specific endonuclease 1 (FEN1) plays a critical role in base excision repair (BER), which is responsible for eliminating various lesions such as oxidative nucleotides and alkylated bases (Lindahl and Wood 1999; Matsuzaki et al. 2002; Tomlinson et al. 2010). Consistent with this, *FEN1*$^{-/-}$ chicken DT40 cells showed sensitivity to oxidative damaging agents (Matsuzaki et al. 2002). If any base lesions escape removal by DNA damage repair prior to DNA replication, the vast majority of base lesions stall replicative DNA polymerases. To overcome this difficulty, cells employ a strategy termed DNA damage tolerance, which includes the employment of translesion DNA synthesis (TLS)

polymerases (Lange et al. 2011). REV1 and DNA polymerase zeta (REV3 and REV7) play critical roles in TLS, and incorporate a nucleotide opposite a lesion rather than repairing it, thereby bypassing the lesion (Lange et al. 2011; Ohmori et al. 2001; Murakumo et al. 2000). Indeed, *REV3*$^{-/-}$DT40 cells were hypersensitive to a wide variety of DNA damaging agents (Sonoda et al. 2003; Okada et al. 2005; Wu et al. 2006; Hirota et al. 2010; Ji et al. 2011b; Liu et al. 2012). Taken together, a defect in FEN1 or REV3 causes stalling of DNA replication, which eventually leads to the formation of DSBs, γH2AX foci, and chromosomal breaks in mitotic cells. It should be noted that the hypersensitivity of *REV3*$^{-/-}$ to chemical compounds suggests their potent mutagenecity in DNA polymerase zeta-expressing normal cells, since DNA polymerase zeta is responsible for the majority of spontaneously arising mutations, at least in the budding yeast (Gibbs et al. 2005).

In the present study, we have transduced a MARCO-TR chimeric transgene in wild-type and mutant strains deficient in base excision repair (*FEN1*$^{-/-}$) and translesion synthesis (*REV3*$^{-/-}$) by retroviral infection and assessed their ability to take up particles. We showed that expression of the chimera significantly enhanced internalization of MWCNTs. Importantly, MWCNTs caused a cytotoxic effect associated with marked increases in the number of mitotic chromosomal aberrations on DT40 cells, and this was greater in the *FEN1*$^{-/-}$and *REV3*$^{-/-}$cells compared to wild-type cells. Based on these results, we propose a novel assay system using the chimera-expressing DT40 strains to screen for CNTs-induced genotoxicity.

Materials and methods

Multi-walled carbon nanotubes (MWCNTs)

MWCNTs prepared using a catalytic chemical vapor deposition (CCVD) method (Bussan Nanotech Research, Ibaraki, Japan) were used. The nominal characteristics of the MWCNTs were as follows: the average and standard deviation for the size of MWCNTs were 7.41 and 2.96 μm, respectively. The suspension of MWCNTs in RPMI 1640 was stable at a concentration of 50 μg/ml, though MWCNTs agglomerated within 2 h at a concentration of 500 μg/ml (Fig. S1). The MWCNTs were heat-treated at 250 °C for 2 h in an electric furnace to remove any contaminating endotoxins and then suspended in 10 % endotoxin-free Pluronic F68 (Sigma, St. Louis, MO, USA). The MWCNT suspension was ultrasonicated and added to cell cultures at a final Pluronic F68 concentration of 1 %.

Cell culture

Wild-type, *FEN1*$^{-/-}$ and *REV3*$^{-/-}$ chicken DT40 mutant strains were used to make chimera-expressing DT40 cells. Chicken DT40 cells were cultured at 39.5 °C in a 5 % CO_2 atmosphere in RPMI 1640 medium supplemented with 10 % heat-inactivated fetal bovine serum (FBS), 1 % chicken serum, 10 μM β-mercaptoethanol, 100 U/ml penicillin, 100 μg/ml streptomycin and 2 μmol/ml L-glutamine.

Chimera construction

The schema used to construct the chimeric genes is illustrated in Fig. S2; restriction sites were engineered into primers to facilitate this. Primer sequences used to construct the transferrin receptor—MARCO chimeric receptor are given in Supplementary Table S1. The 5′ region of the transferrin receptor cDNA was amplified using primers P1 and P2 and ligated into the pTOPO vector (Invitrogen). Similarly, the 3′ region of MARCO was amplified using primers P3 and P5 for the long chimera and P4 and P5 for the short chimera and ligated into pTOPO. The 5′ region of the transferrin receptor cDNA was ligated into the corresponding sites of pTOPO containing the 3′ region of MARCO to create MARCO-TR chimera (Fig. S2). The plasmid was extracted using the standard plasmid purification methods. This plasmid was digested with BamHI and MfeI to liberate the full-length chimeric gene. This chimera was cloned into the pMSCV retroviral expression vector (Clontech). The newly engineered retroviral expression vector was co-transfected into human 293T cells with a helper plasmid (pClampho) expressing gag, pol, and env genes to produce viral supernatant.

Construction of chimera-expressing DT40 strains

The viral supernatant was collected after 24 h and used to transduce wild-type, *FEN1*$^{-/-}$ and *REV3*$^{-/-}$ DT40 mutant strains. The efficiency of each step was assessed by quantifying the number of cells expressing GFP. These strains were assessed for their ability to efficiently take up particles.

Adherence assay

Adherence of these strains was evaluated using the WST-8 cell counting kit (Dojindo, Osaka, Japan), a modified MTT (3-(4,5-dimethylthiazol-2-yl)-2,5-diphenyltetrazolium bromide) assay method. DT40 cells were cultured at 2.5×10^6 cells/ml in a 6-well plate with 4-ml fresh media. After incubating for 1 h, each well was washed twice with 1 ml PBS and the cells remaining on the bottom of

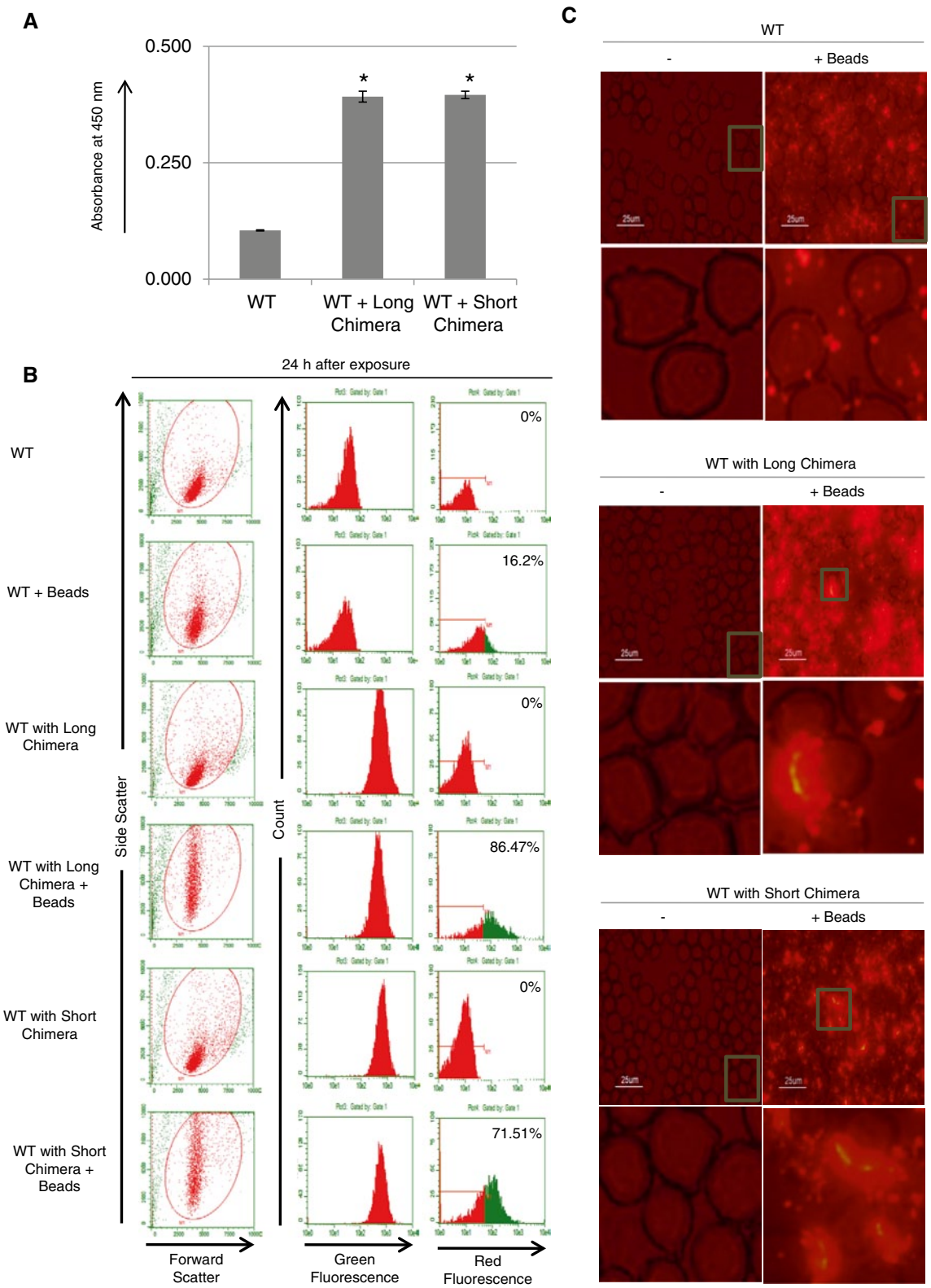

the dish were incubated for 1 h with WST-8 diluted with phenol red-free RPMI 1640. After the incubation, a 150-µl WST-8 solution was mixed with 0.1 N HCl solution (15 µl) to stop the reaction in a 96-well plate and the absorbance at 450 nm was measured using a microplate reader (POLARstar OPTIMA, BMG Labtech, Ortenberg, Germany). The absorbance is proportional to the number of living cells.

◀ **Fig. 4** Chicken DT40 cells stably expressing MARCO-TR recognize both the culture dish surface and polystyrene particles. **a** Chicken DT40 cells stably expressing MARCO-TR chimeras can adhere to the bottom of the polystyrene dish. DT40 cells of the indicated genotypes were incubated for 1 h at 39.5 °C. After removing media, each well was washed with PBS twice and the number of cells was evaluated using the WST-8 Cell Counting Kit (MTT assay), where the absorbance is directly proportional to the number of living cells adhered to the bottom of the dish. *Significantly different from control value. **b** DT40 cells of the indicated genotypes stably either expressing or not expressing MARCO-TR receptor were exposed to 200-nm red fluorescent microspheres for 24 h. The cellular association of microspheres was evaluated by flow cytometry. Cells expressing the MARCO-TR receptor can take up particles, and the fluorescence intensity increases with time. **c** Chicken DT40 cells stably either expressing or not expressing MARCO-TR were incubated with 200-nm red fluorescent microspheres for 24 h. After incubation, cells were washed three times with medium and then suspended in fresh medium. The cells associated with particles were observed using fluorescence microscopy. The *lower panels* show a higher magnification of the *boxed* region from the *upper panels*. The amount of associated beads increased with time and cells expressing MARCO-TR receptors associated with larger number of particles

Measurement for cellular association of particles by flow cytometry

DT40 cells expressing the MARCO-TR chimeric receptor were plated at 0.5×10^6 cells/ml with 2-ml fresh media in a 24-well plate. The cells were exposed to 200-nm red fluorescent microspheres (Red FluoSphere® 200, Ex/Em 580/605 nm, Molecular Probes-Life Technology, Eugene, OR) at a final concentration of 4.5×10^8 particles/ml. The intensity of fluorescence in the cellular fraction was analyzed at 3 and 24 h after addition of the microspheres by flow cytometry (Guava easyCyte 8HT, Millipore, Hayward, CA). The flow cytometric analysis was performed twice and 5,000 events were counted per experiment. Representative pictures were taken from the same experiment.

In a different experiment, we used pyrogen-free Pluronic F68 to disperse MWCNTs in the culture medium at a final concentration of 1 %, since detergents or additives have been used to disperse CNTs for toxicological studies. The MWCNT suspension in the culture medium (5 μg/ml) appeared to be stable and MWCNTs did not agglomerate greatly in 12 h in the presence of the Pluronic surfactant. The cellular association of MWCNTs was evaluated by measuring changes in side-scattering intensity using flow cytometry.

Fluorescence microscopy

DT40 cells expressing the MARCO-TR receptor were suspended at 0.5×10^6 cells/ml in culture medium and cultured with 200-nm red fluorescent microspheres (polystyrene beads) for 3 and 24 h in 24-well plates. DT40 cells without the MARCO-TR receptor were used as negative controls. An aliquot of the cell suspension was cytocentrifuged on glass slides and the association of fluorescent microspheres with the cells was observed by fluorescence microscopy.

Cellular viability assay

Chicken DT40 cells were suspended in culture medium at 1×10^6 cells/ml and cultured in the presence or absence of MWCNTs (2 μg/ml, 5 μg/ml and 10 μg/ml) for 12 h at 39.5 °C. Negative control cells were exposed to 1 % Pluronic F68 detergent alone. After 12 h, the cell viability was measured with the trypan blue dye exclusion assay using a hemocytometer.

Immunostaining assay for 8-OH-dG positive cells

Chicken DT40 cells were suspended in culture medium at 1×10^6 cells/ml and cultured in the presence or absence of 5 μg/ml MWCNTs for 12 h at 39.5 °C. After 12 h, cells were smeared on glass slides using a cytospin and were fixed using Bouin solution for 10 min. After washing with PBS, cells were permeabilized with 0.2 % Triton X-100 for 5 min. After washing again with PBS, cells were incubated for 20 min with blocking solution (3 drops of horse serum in 10 ml PBS). Cells were incubated with a mouse anti-8-OH-dG antibody (N45.1, JalCA, Shizuoka, Japan) for 30 min. Immunostaining was completed according to the instructions supplied with the Vectastain® Elite mouse ABC kit (Vector Lab, Burlingame, CA). Finally, 8-OH-dG in the nuclei was visualized using a Vectastain® DBA kit.

Measurement of γH2AX foci

To evaluate the differential induction of DNA double-strand breaks by MWCNTs in the DT40 strains, we determined the number of γH2AX foci in nuclear DNA. Chicken DT40 cells were suspended in culture medium at 1×10^6 cells/ml and cultured in the presence or absence of 5 μg/ml MWCNTs for 12 h at 39.5 °C. Experimental conditions for immunocytochemical analysis were as described previously (Takata et al. 2001). Briefly, cells were applied to a glass slide using a cytospin and fixed using 1 % paraformaldehyde (Nacalai Tesque, Kyoto, Japan) for 10 min at room temperature and rinsed with PBS. Cells were permeabilized for 10 min in 0.1 % NP40/PBS (Nonidet P-40, NacalaiTesque, Kyoto, Japan) and rinsed with PBS. After blocking with 3 % BSA/PBST (bovine serum albumin F–V, pH 5.2), the cells were treated with specific primary anti-γH2AX monoclonal mouse antibodies (1:500, Millipore, Billerica, MA) for

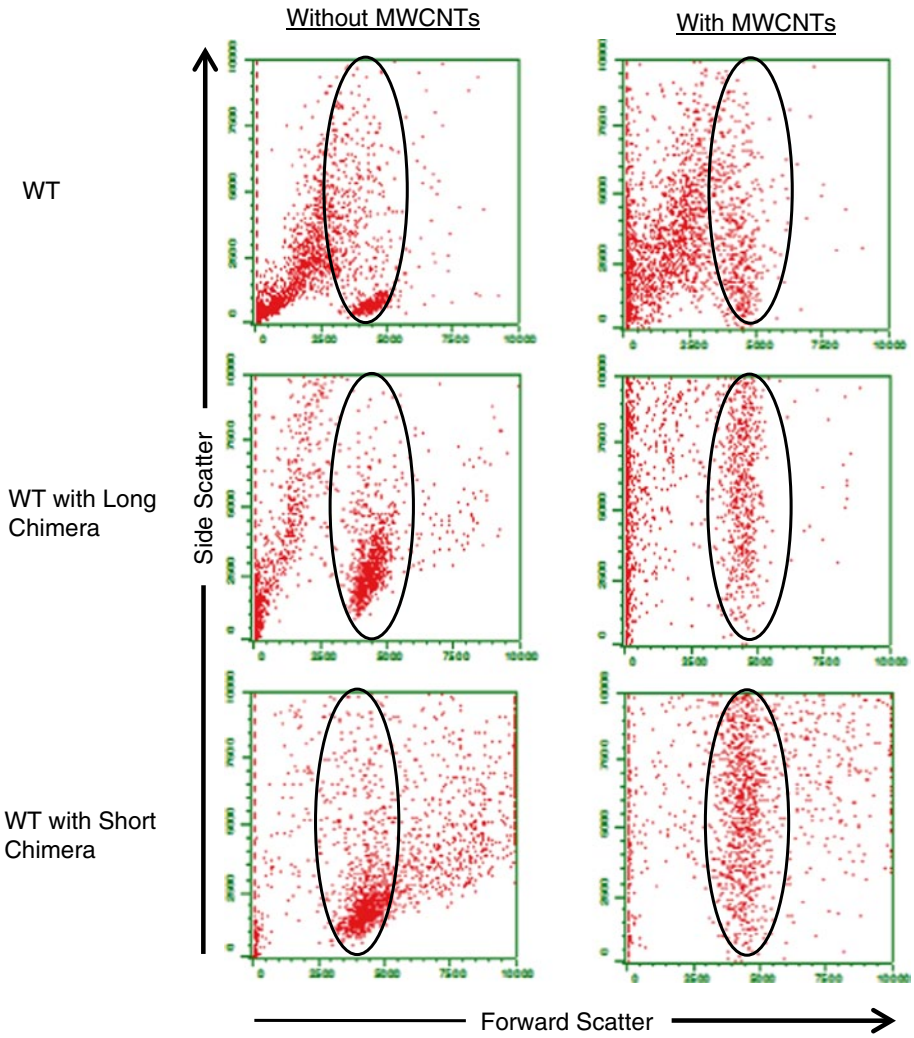

Fig. 5 Chicken DT40 cells stably expressing MARCO-TR uptake MWCNTs efficiently. DT40 cells of the indicated genotypes were cultured in the presence (*right panel*) or absence (*left panel*) of MWCNTs for a pre-determined time (12 h) and analyzed using flow cytometry. Cells expressing MARCO-TR associated more efficiently with MWCNTs and became denser. As a consequence, these cells demonstrated greater side scatter (SSC)

60 min under humidified conditions at 37 °C, followed by secondary Alexa 488-conjugated anti-mouse IgG antibodies (1:500, Molecular Probes, Eugene, OR) for 40 min and were thoroughly washed with PBS. The nuclei of at least 100 morphologically intact cells were examined for each group and the numbers of γH2AX foci were counted using fluorescence microscopy.

Chromosomal aberration analysis

Chicken DT40 cells were suspended in culture medium at 1×10^6 cells/ml and cultured in the presence or absence of 5 μg/ml MWCNTs for 9 h at 39.5 °C. The cells were treated with 0.1 μg/ml colcemid (GIBCO-BRL, Grand Island, NY) for the last 3 h before being harvested. Experimental conditions for chromosomal aberration analysis were as described previously (Sonoda et al. 1998). Briefly, harvested cells were treated with 1 ml of 75 mM KCl for 15 min at room temperature and fixed in 5 ml of a freshly prepared 3:1 mixture of methanol/acetic acid. The cell suspension was dropped onto an ice-cold wet glass slide and air-dried. The slides were stained with 5 % Giemsa solution (NacalaiTesque) for 10 min and air-dried after being rinsed carefully with water. All chromosomes in each mitotic cell were scored at 1,000× magnification. A total of 50 mitotic cells were scored for each group using a microscope.

Statistical analysis

Data are presented as means ± SEM of three independent experiments. Statistical analyses were performed by ANOVA followed by Bonferroni—Holm's post hoc analysis. The statistical significance level was set at $p < 0.05$.

Results

The chicken DT40 B lymphocyte cell line does not efficiently incorporate particles even when the macrophage receptor (MARCO) is expressed

To analyze genotoxicity of particles, we first investigated whether or not DT40 cells took up particles. To this end, we exposed DT40 cells to 200-nm red fluorescent microspheres (polystyrene beads) for 24 h, and evaluated uptake of the particles using flow cytometric analysis. The fluorescent beads only poorly associated with DT40 cells, regardless of the incubation time (Fig. 1). We postulated that defective uptake of the fluorescent beads by DT40 cells was attributable to their absence of a cell surface receptor for particles.

To increase the uptake of particles, we integrated the full-length MARCO gene in chicken DT40 cells by retroviral infection (Fig. 2a, b) and assessed the ability of these cells to take up particles. The efficiency of the infection was assessed by quantifying the percentage of cells expressing GFP (Fig. 2c). Several previous studies showed the involvement of MARCO in the cellular uptake of polystyrene particles, including nanoparticles (Kanno et al. 2007). Although chicken DT40 cells expressing full-length MARCO attached to the bottom of a culture dish (Fig. 2d), the cells did not internalize the particles efficiently (Fig. 2e). These results indicate that MARCO-expressing DT40 cells may efficiently bind particles but are unable to internalize them. We postulated that the defective internalization may be attributable to poor functioning of the transmembrane and cytoplasmic domains of MARCO, which are required for MARCO-mediated internalization of particles by macrophages.

Construction of DT40 strains expressing the MARCO-TR chimera

To generate a functional MARCO receptor, we replaced the trans-membrane and cytoplasmic domains of MARCO with the corresponding domains derived from the transferrin receptor. We chose it because it functions in all cell types. Transferrin is a carrier protein for iron and facilitates constitutive clathrin-mediated endocytosis in vertebrates (Aisen and Listowsky 1980; Newman et al. 1982). The transferrin-iron complex binds to the transferrin receptor, and is subsequently internalized (Goldstein et al. 1979; Hopkins and Trowbridge 1983; Dautry-Varsat et al. 1983). We constructed chimeric receptors consisting of the trans-membrane and cytoplasmic domains of the transferrin receptor and the extra-cellular domain of MARCO (MARCO-TR chimera genes).

To generate the chimeric receptor, we identified the chicken MARCO and transferrin receptor (TFRC) gene orthologues by searching the HomoloGene database at the NCBI (www.ncbi.nlm.nih.gov) using these gene names as search terms. The mRNA sequences obtained were used to interrogate the BLAT chicken server (www.genome.ucsc.edu). The conserved YTRF motif, which is responsible for constitutive clathrin-mediated endocytosis, is located within the 5′ region of the transferrin receptor gene (Fig. S3). The cysteine-rich scavenger receptor domain of MARCO, which is important for ligand binding, is located at the 3′ region of the MARCO gene (Elomaa et al. 1995). We then constructed two different chimeras. The long chimera consists of the 5′ region of the transferrin receptor gene fused to the collagen triple helix and cysteine-rich scavenger domains of MARCO. The short chimera consists of the 5′ region of the transferrin receptor gene fused to the cysteine-rich scavenger domain, but not the collagen triple helix domain, of MARCO (Figs. 3a, b, S2A, S2B).

These chimeras were engineered into the pMSCV retroviral expression vector, which can simultaneously express GFP and the chimeric gene. The newly engineered retroviral expression vectors were used to produce viral particles, which were used to infect wild-type (WT), *FEN1*$^{-/-}$ and *REV3*$^{-/-}$DT40 mutant strains. The efficiency of the infection was assessed by quantifying the percentage of cells expressing GFP (Figs. 3c, S2C).

Chicken DT40 cells stably expressing the chimera recognize the surface of the culture dish and efficiently take up polystyrene particles and MWCNTs

To confirm the expression of the MARCO-TR chimeras in DT40 cells, we investigated the adhesion of cells to a plastic culture dish. This adhesion assay showed that stable expression of both long and short chimeras on chicken DT40 cells resulted in their adherence to the bottom of plastic dishes (Fig. 4a), indicating that both chimeras are functionally expressed. Next, we investigated the association of 200-nm red fluorescent microspheres (polystyrene beads) with chimera-expressing DT40 cells. Flow cytometric analysis showed that the red fluorescent beads preferentially associated with GFP-positive DT40 cells stably expressing long and short chimeras in a time-dependent manner (Figs. 4b, S4A, S4B). Moreover, cells with increased side scatter displayed stronger red fluorescence signals, where side scatter depends on the density of intracellular particles such as cytoplasmic granules. DT40 cells not expressing the chimera were used as a negative control, and no obvious association of polystyrene beads was found in this case (Figs. S4A, S4B). Furthermore, the association of polystyrene particles with both long and short chimera-expressing DT40 cells was observed by fluorescence

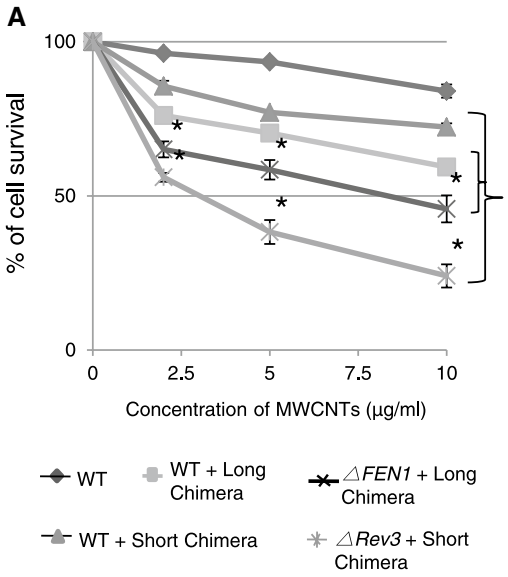
A
100
50
0
% of cell survival
0
2.5
5
7.5
10
Concentration of MWCNTs (μg/ml)
WT
WT + Long Chimera
△FEN1 + Long Chimera
WT + Short Chimera
△Rev3 + Short Chimera

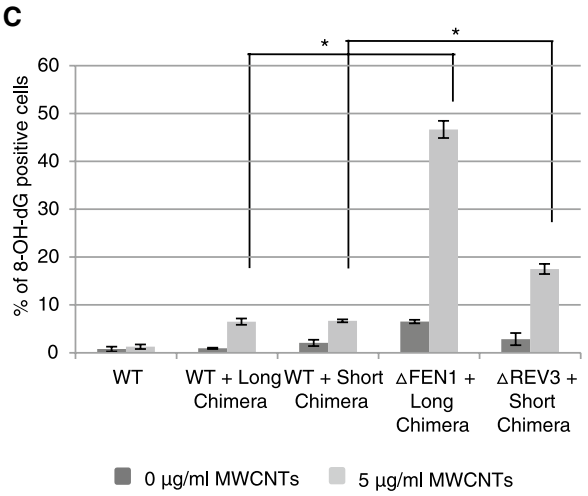
C
60
50
40
30
20
10
0
% of 8-OH-dG positive cells
WT
WT + Long Chimera
WT + Short Chimera
△FEN1 + Long Chimera
△REV3 + Short Chimera
0 μg/ml MWCNTs
5 μg/ml MWCNTs

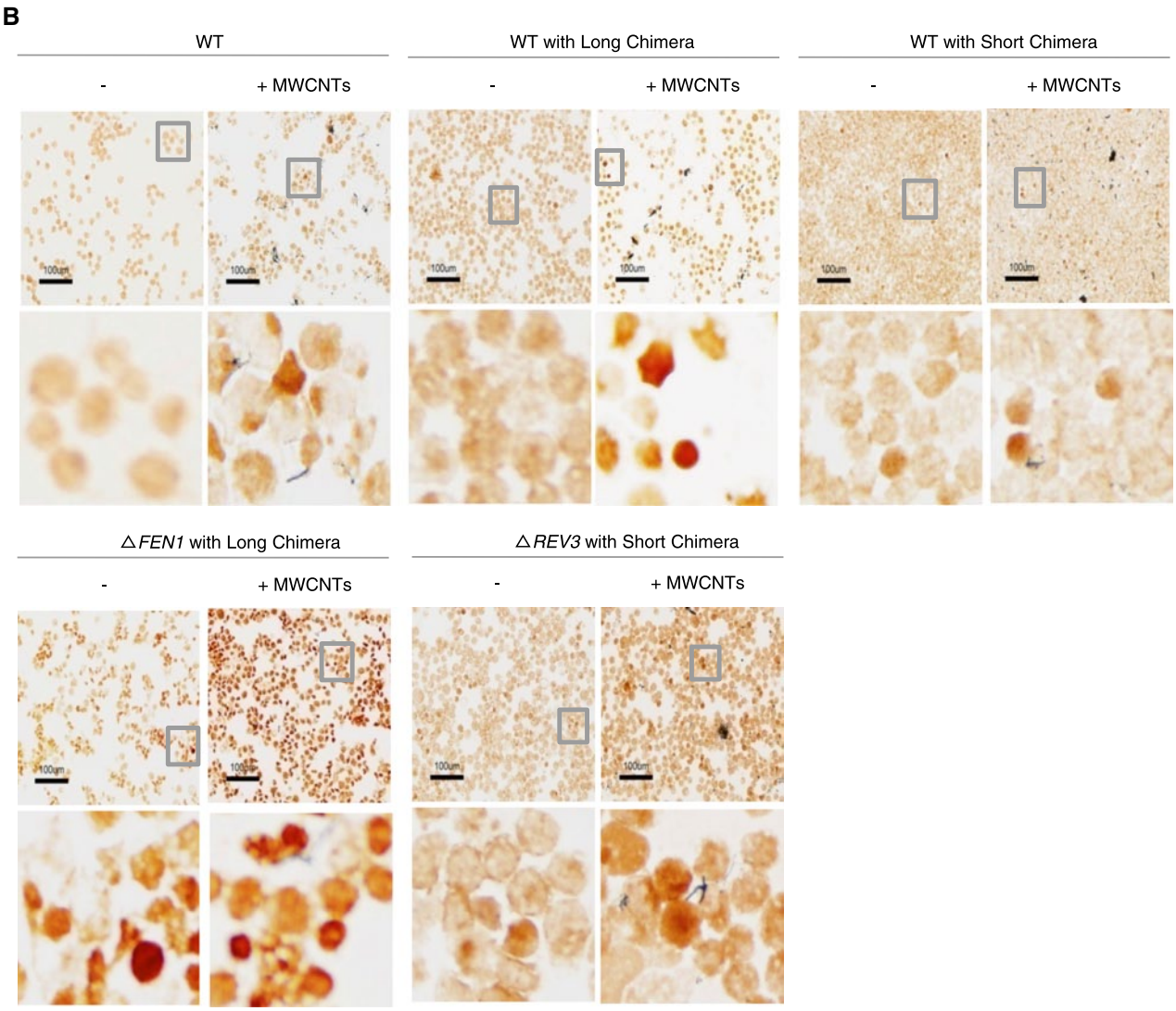
B
WT
WT with Long Chimera
WT with Short Chimera
△FEN1 with Long Chimera
△REV3 with Short Chimera
-
+ MWCNTs

◀**Fig. 6** Cytotoxic and genotoxic effects of multi-walled carbon nanotubes (MWCNTs) in DT40 cells. **a** Cellular tolerance of MARCO-TR chimera-expressing DT40 cells to MWCNTs. DT40 cells of the indicated genotypes were cultured in the presence or absence of MWCNTs for a pre-determined time (12 h). Cell viability was evaluated by trypan blue dye exclusion assay. *Significantly different from control value. **b** Microscopic images of 8-OH-dG lesions (*brown spots*) in MWCNT-treated DT40 cells. MWCNTs induce oxidative damage (8-OH-dG lesions) in chicken DT40 cells. DT40 cells stably expressing or not expressing MARCO-TR chimeras were incubated with or without 5 μg/ml MWCNTs for 12 h. After incubation, cells were cytocentrifuged on glass slides and were immunostained with an anti-8-OH-dG antibody. The *lower panels* show a higher magnification of the *boxed* region from the *upper panels*. **c** Quantification of 8-OH-dG positive cells was performed by counting a total of 500 cells per sample and is shown as the percentage of 8-OH-dG positive cells. *Significantly different from control value

microscopy (Figs. 4c, S4C). These results suggest that chimera-expressing DT40 cells are capable of efficiently taking up the polystyrene particles.

To test the efficiency of MWCNT uptake by chimera-expressing DT40 cells, the engineered strains were exposed to MWCNTs. It should be noted that since MWCNTs are hydrophobic in nature, we used pyrogen-free Pluronic F68 to disperse MWCNTs in the culture medium at a final concentration of 1 %. Following exposure, the cellular association of MWCNTs was evaluated by measuring changes in side-scattering intensity using flow cytometry. The expression of either long or short chimera caused a dramatic increase in the side-scattering intensity in comparison with non-expressing cells (Fig. 5). These findings suggest that only cells expressing a chimera took up MWCNTs rapidly. Taken together, chimera-expressing chicken DT40 cells are capable of recognizing both the surface of the plastic culture dish and polystyrene particles, and take up MWCNTs proficiently.

MWCNTs have greater cytotoxic and genotoxic effects on DNA-repair-deficient cells compared to wild-type cells

This experiment was designed to investigate the cytotoxic effects of MWCNTs on DT40 cells. Chimera-expressing wild-type cells took up MWCNTs efficiently and showed sensitivity to MWCNTs in a dose-dependent manner (Fig. 6a). Wild-type cells expressing the long chimera tended to be more sensitive to MWCNTs than were those expressing the short chimera. Interestingly, the cytotoxic effect of MWCNTs was greater in *FEN1*$^{-/-}$ cells compared to wild-type cells, indicating that MWCNTs may cause DNA damage that cannot be fully repaired by repair-deficient *FEN1*$^{-/-}$ cells, leading to cell death.

To determine the mechanism of cytotoxicity caused by the MWCNTs, we next investigated whether MWCNTs caused oxidative damage to DNA. To this end, we analyzed the formation of the guanine adduct 8-hydroxy deoxyguanosine (8-OH-dG), which significantly contributes to carcinogenesis (Kasai and Nishimura 1984; Jiang et al. 2008; Nagai et al. 2011; Ock et al. 2012). The cells were exposed to MWCNTs, fixed, and immunostained with an anti-8-OH-dG antibody, and the number of 8-OH-dG-positive cells was calculated. The number of 8-OH-dG-positive cells was significantly higher in wild-type DT40 cells stably expressing the chimeric receptors when treated with MWCNTs compared to untreated cells (Fig. 6b, c). Notably, MWCNTs were also associated with DT40 cells not expressing the chimera and did cause 8-OH-dG lesions in DNA, but these processes were slower and the number of 8-OH-dG lesions was much smaller than for chimera-expressing DT40 cells. These observations demonstrated that the short and long MARCO-TR receptors significantly facilitate the uptake of MWCNTs. Importantly, we found an increased number of 8-OH-dG-positive cells when DNA-repair-deficient strains were expressing the chimeric receptor, and this was particularly dramatic for *FEN1*$^{-/-}$ DT40 cells. Enhanced 8-OH-dG in *REV3*$^{-/-}$ cells suggests that DNA polymerase zeta may be involved in elimination of oxidative base damage, as are other TLS polymerases (Yoshimura et al. 2006).

To evaluate the induction of DNA double-strand breaks (DSBs) by MWCNTs, we measured the number of subnuclear phosphorylated histone H2AX (γH2AX) foci (Rogakou et al. 1999; Lobrich et al. 2010). Chicken DT40 cells were cultured in the absence or presence of 5 μg/ml MWCNTs for 6 h at 39.5 °C. The immunofluorescence analysis of γH2AX foci suggested that MWCNTs significantly induced DSBs in DT40 cells. The induction of DSBs in DNA damage repair-deficient cells was significantly greater than in repair-proficient cells (Fig. 7), consistent with the findings that FEN1 and REV3 are important for preventing the occurrence of DSBs during DNA replication.

Finally, we attempted to identify whether MWCNT-treated cells exhibited chromosomal aberrations in mitotic cells (Takata et al. 1998; Yamazoe et al. 2004). To address this, chicken DT40 cells were cultured in the presence or absence of 5 μg/ml MWCNTs for 9 h and cells were treated with colcemid for the last 3 h to cause mitotic arrest. Figure 8 shows that MWCNTs induced significantly increased numbers of both isochromatid- and chromatid-type chromosomal breaks in wild-type mitotic cells expressing the chimera compared to those not expressing the chimera (Fig. 8). Very importantly, MWCNT-induced chromosomal aberrations were dramatically increased in repair-deficient *FEN1*$^{-/-}$ and *REV3*$^{-/-}$ chicken DT40 mutant strains compared to repair-proficient WT DT40 cells (Fig. 8a–d), indicating that MWCNT treatment also affects chromatin integrity by inducing DNA damage and thereby interferes with DNA replication.

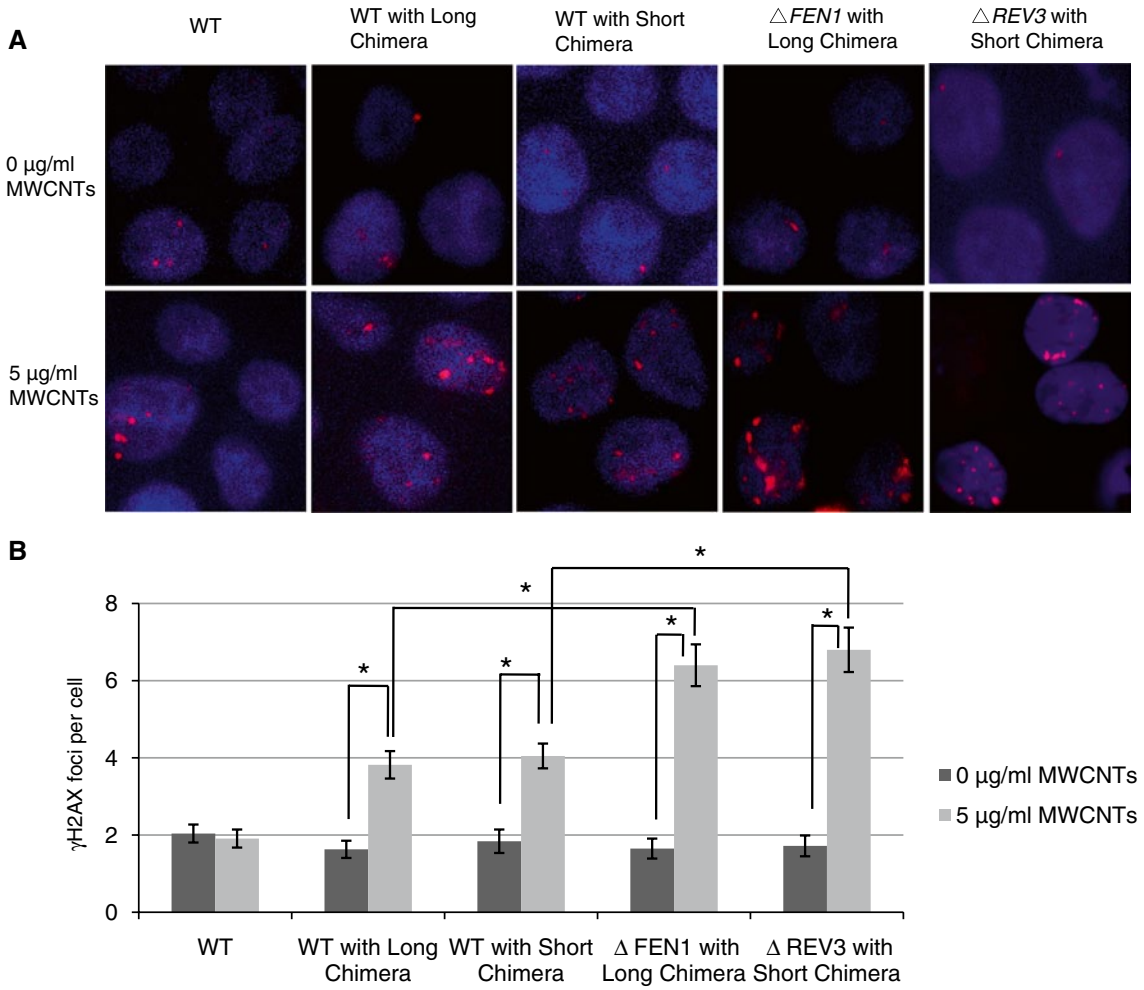

Fig. 7 Formation of γH2AX foci is increased in MARCO-TR chimera-expressing DT40 cells after exposure to MWCNTs. **a** Fluorescence microscopic images of γH2AX foci formation. DT40 cells of the indicated genotypes were cultured in the absence (*upper panel*) or presence (*lower panel*) of MWCNTs. The analysis of γH2AX focus formation per cell was carried out in these cells after incubation for 6 h with MWCNTs. **b** Quantification of γH2AX foci formation after 6 h treatment with MWCNTs. At least 100 cells were counted per condition in each experiment. *Significantly different from control value

Discussion

In this study, we used the chicken DT40 B lymphoid cell line to develop a novel bio-assay to detect particle- and nanoparticle-induced genotoxicity. We found that DT40 cells only poorly internalized particles, and thus could not be used for high throughput screening of particle- and nanoparticle-induced genotoxicity, since the assay must be extremely sensitive due to the very limited exposure time of cells to particles or nanoparticles. We circumvented this requirement by engineering a chimeric trans-membrane receptor (MARCO-TR) carrying the trans-membrane and cytoplasmic portion of the transferrin receptor. The cytoplasmic portion includes the YTRF motif, a signal enhancing endocytosis of the transferrin receptor (Collawn et al. 1993). We assessed the internalization of MWCNTs by chimera-expressing chicken DT40 cells by increases in side-scattering intensity using flow cytometry. We then confirmed the internalization by detecting the induction of oxidative base damage (8-OH-dG) of genomic DNA, an observation that agrees with previous studies (Kang et al. 2008a, b). We therefore conclude that expression of transgenic MARCO-TR greatly facilitates efficient internalization of particles and nanoparticles, including MWCNTs, by DT40 cells.

The expression of MARCO-TR may allow for internalization of a wide variety of particles and nanoparticles by DT40 cells. In fact, here, we showed that MARCO-TR-expressing DT40 cells efficiently took up both 200-nm red fluorescent microspheres (polystyrene beads) and MWCNTs. We can easily express MARCO-TR to the same extent on different gene-disrupted mutant DT40 clones because

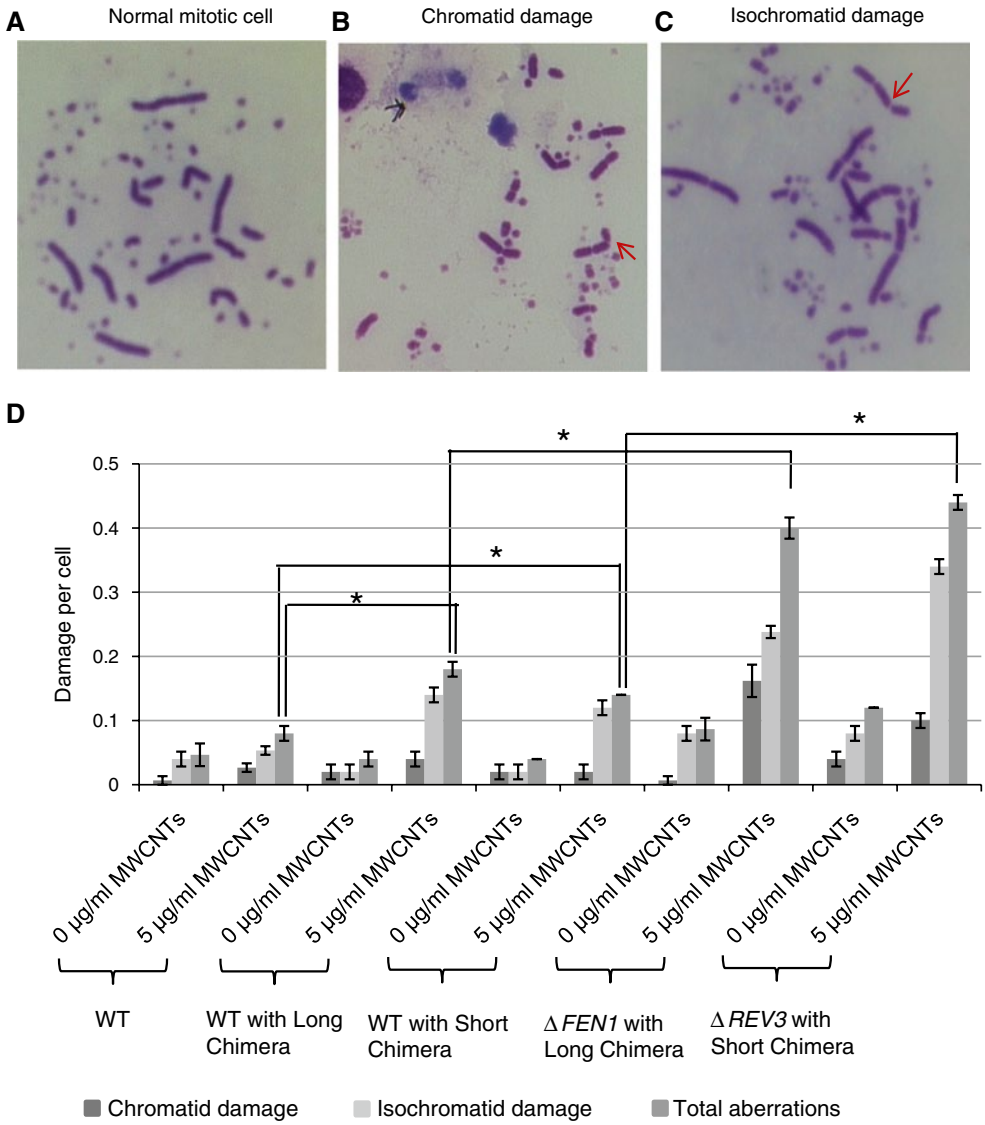

Fig. 8 Chromosomal aberration is increased in MARCO-TR chimera-expressing DT40 cells after exposure to MWCNTs. (**a**–**c**) Representative karyotype analysis of chicken DT40 cells stably expressing MARCO-TR chimera in a normal mitotic cell (**a**) or with chromatid damage (**b**) or isochromatid damage (**c**). The analysis of chromosomal damage was carried out in these cells after incubation for 9 h with MWCNTs and with colcemid for the last 3 h. (**d**) Quantification of chromosomal aberration after 9 h treatment with MWCNTs. DT40 cells of the indicated genotypes were cultured in the presence or absence of MWCNTs. At least 50 mitotic cells were counted per condition in each experiment. *Significantly different from control value

we can efficiently transduce the MARCO-TR transgene through retroviral infection and accurately quantitate expression of MARCO-TR (Fig. 3c). Thus, MARCO-TR-expressing DT40 mutant clones carrying defects in various biochemical pathways can be used for evaluating genotoxicity caused by particles and nanoparticles in the future. An unsolved question is the quaternary structure formed by multimerization of our chimera, because the transferrin receptor ordinarily forms a disulfide-bonded dimer (Sutherland et al. 1981) while MARCO has a trimeric structure (Matsumoto et al. 1990). Taking into account the fact that MWCNTs are hydrophobic in nature, our data suggest that MARCO-TR expressing DT40 cells may be able to efficiently take up particles and nanoparticles having a wide variety of physical characteristics.

We previously characterized the nature of DNA lesions induced by test chemical compounds (Nojima et al. 2005; Evans et al. 2010; Ji et al. 2011a, b; Murai et al. 2012 Liu et al. 2012). Both DNA-repair-deficient *FEN1*$^{-/-}$ and TLS-deficient *REV3*$^{-/-}$ clones showed greater sensitivity to MWCNTs compared to wild-type cells (Fig. 6a). Interestingly, *FEN1*$^{-/-}$ cells showed less sensitivity to MWCNTs than *REV3*$^{-/-}$ cells (Fig. 6a), while *FEN1*$^{-/-}$ cells showed greater amounts of 8-OH-dG compared to *REV3*$^{-/-}$ cells

following exposure to MWCNTs (Fig. 6c). Moreover, MWCNTs induced mitotic chromosomal breaks in *FEN1*$^{-/-}$ and *REV3*$^{-/-}$ cells to the same extent (Fig. 8d). Presumably, MWCNTs cause oxidative stress as evidenced by the accumulation of 8-OH-dG in genomic DNA. 8-OH-dG is eliminated by the FEN1-dependent base excision repair pathway, while unrepaired lesions interfere with DNA replication leading to the formation of γH2AX subnuclear foci (Fig. 7) and chromosomal breaks in mitotic cells (Fig. 8). This conclusion agrees with the previous findings that nanoparticles induce cellular toxicity via both oxidative stress-dependent and independent pathways (Shvedova et al. 2012; Nagai et al. 2011; Jiang et al. 2008). Oxidative stress is the dominant carcinogenic mechanism for most toxic nanoparticles (Donaldson and Tran 2002). Accordingly, nanoparticles cause malignancy through two distinct mechanisms. First, oxidized nucleotides result in the accumulation of point mutations. The second mechanism is that oxidative stress triggers inflammation via oxidative stress-responsive transcription factors (Donaldson and Tran 2002) and chronic inflammation significantly contributes to carcinogenesis (Karin et al. 2002; Mantovani et al. 2008; Polk and Peek 2010). It remains unsolved whether MWCNTs induce several different types of genetic lesions other than oxidative base damage.

In summary, we showed that chimera-expressing chicken DT40 cells are able to efficiently internalize both polystyrene particles and MWCNTs in a time-dependent manner. MWCNTs taken up by DT40 cells showed a cytotoxic effect, which was more dramatic in DNA damage repair-deficient cells than in wild-type cells. Furthermore, MWCNT-induced oxidative damage (8-OH-dG formation) was higher in repair-deficient cells compared to repair-proficient cells. Finally, a greater number of both γH2AX foci and mitotic chromosomal aberrations, indicators of DSBs, were observed in repair-deficient cells. Thus, this study provides proof of principle that our experimental system is well suited to the sensitive screening of genotoxic nanomaterials such as CNTs.

Acknowledgments We thank the members of the S. T. laboratory and S. H. laboratory for help and support. This research was supported by grants-in-aid for scientific research from the Ministry of Education, Culture, Sports, Science and Technology, Japan.

Conflict of interest There is no conflict of interest to declare.

References

Aisen P, Listowsky I (1980) Iron transport and storage proteins. Annu Rev Biochem 49:357–393

Arredouani M, Yang Z, Ning Y, Qin G, Soininen R, Tryggvason K, Kobzik L (2004) The scavenger receptor MARCO is required for lung defense against pneumococcal pneumonia and inhaled particles. J Exp Med 200:267–272

Buerstedde JM, Takeda S (1991) Increased ratio of targeted to random integration after transfection of chicken B cell lines. Cell 67:179–188

Collawn JF, Lai A, Domingo D, Fitch M, Hatton S, Trowbridge IS (1993) YTRF is the conserved internalization signal of the transferrin receptor, and a second YTRF signal at position 31–34 enhances endocytosis. J Biol Chem 268:21686–21692

Cui D, Tian F, Ozkan CS, Wang M, Gao H (2005) Effect of single wall carbon nanotubes on human HEK293 cells. Toxicol Lett 155:73–85

Dautry-Varsat A, Ciechanover A, Lodish HF (1983) pH and the recycling of transferrin during receptor-mediated endocytosis. Proc Natl Acad Sci USA 80:2258–2262

Donaldson K, Tran CL (2002) Inflammation caused by particles and fibres. Inhal Toxicol 14:5–27

Donaldson K, Aitken R, Tran L, Stone V, Duffin R, Forrest G, Alexander A (2006) Carbon nanotubes: a review of their properties in relation to pulmonary toxicology and workplace safety. Toxicol Sci 92:5–22

Elomaa O, Kangas M, Sahlberg C, Tuukkanen J, Sormunen R, Liakka A, Thesleff I, Kraal G, Tryggvason K (1995) Cloning of a novel bacteria-binding receptor structurally related to scavenger receptors and expressed in a subset of macrophages. Cell 80:603–609

Elomaa O, Sankala M, Pikkarainen T, Bergmann U, Tuuttila A, Raatikainen-Ahokas A, Sariola H, Tryggvason K (1998) Structure of the human macrophage MARCO receptor and characterization of its bacteria-binding region. J Biol Chem 273:4530–4538

Evans TJ, Yamamoto KN, Hirota K, Takeda S (2010) Mutant cells defective in DNA repair pathways provide a sensitive high-throughput assay for genotoxicity. DNA Repair 9:1292–1298

Gibbs PE, McDonald J, Woodgate R, Lawrence CW (2005) The relative roles in vivo of Saccharomyces cerevisiae Polη, Polζ, Rev1 protein and Pol32 in the bypass and mutation induction of an abasic site, T-T (6–4) photoadduct and T-T cis-syn cyclobutane dimer. Genetics 169:575–582

Goldstein JL, Anderson RG, Brown MS (1979) Coated pits, coated vesicles, and receptor-mediated endocytosis. Nature 279:679–685

Greaves DR, Gordon S (2005) Recent insights into the biology of macrophage scavenger receptors. J Lipid Res 46:11–20

Hirano S, Kanno S, Furuyama A (2008) Multi-walled carbon nanotubes injure the plasma membrane of macrophages. Toxicol Appl Pharmacol 232:244–251

Hirano S, Fujitani Y, Furuyama A, Kanno S (2010) Uptake and cytotoxic effects of multi-walled carbon nanotubes in human bronchial epithelial cells. Toxicol Appl Pharmacol 249:8–15

Hirano S, Fujitani Y, Furuyama A, Kanno S (2012) Macrophage receptor with collagenous structure (MARCO) is a dynamic adhesive molecule that enhances uptake of carbon nanotubes by CHO-K1 cells. Toxicol Appl Pharmacol 259:96–103

Hirota K, Sonoda E, Kawamoto T, Motegi A, Masutani C, Hanaoka F, Szuts D, Iwai S, Sale JE, Lehmann A, Takeda S (2010) Simultaneous disruption of two DNA polymerases, Polη and Polζ, in Avian DT40 cells unmasks the role of Polηin cellular response to various DNA lesions. PLoS Genet 6(10):e1001151

Hopkins CR, Trowbridge IS (1983) Internalization and processing of transferrin and the transferrin receptor in human carcinoma A431 cells. J Cell Biol 97:508–521

Ji K, Kogame T, Choi K, Wang X, Lee JY, Taniguchi Y, Takeda S (2009) A novel approach using DNA repair-deficient chicken DT40 cell lines for screening and characterizing the genotoxicity of environmental contaminants. Environ Health Perspect 117:1737–1744

Ji K, Choi K, Giesy JP, Takeda S (2011a) Genotoxicity of several polybrominated diphenyl ethers (PBDEs) and hydroxylated PBDEs, and their mechanisms of toxicity. Environ Sci Technol 45:5003–5008

Ji K, Seo J, Liu X, Lee J, Lee S, Lee W, Park J, Khim JS, Hong S, Choi Y, Shim WJ, Takeda S, Giesy JP, Choi K (2011b) Genotoxicity and endocrine disruption potentials of sediment near an oil spill site: two years after the Hebei Spirit oil spill. Environ Sci Technol 45:7481–7488

Jia G, Wang H, Yan L, Wang X, Pei R, Yan T, Zhao Y, Guo X (2005) Cytotoxicity of carbon nanomaterials: single-wall nanotube, multi-wall nanotube, and fullerene. Environ Sci Technol 39:1378–1383

Jiang L, Nagai H, Ohara H, Hara S, Tachibana M, Hirano S, Shinohara Y, Kohyama N, Akatsuka S, Toyokuni S (2008) Characteristics and modifying factors of asbestos-induced oxidative DNA damage. Cancer Sci 99:2142–2151

Kagan VE, Tyurina YY, Tyurin VA, Konduru NV, Potapovich AI, Osipov AN, Kisin ER, Schwegler-Berry D, Mercer R, Castranova V, Shvedova AA (2006) Direct and indirect effects of single walled carbon nanotubes on RAW 264.7 macrophages: role of iron. Toxicol Lett 165:88–100

Kang S, Herzberg M, Rodrigues DF, Elimelech M (2008a) Antibacterial effects of carbon nanotubes: size does matter. Langmuir 24:6409–6413

Kang S, Mauter MS, Elimelech M (2008b) Physicochemical determinants of multi-walled carbon nanotube bacterial cytotoxicity. Environ Sci Technol 42:7528–7534

Kanno S, Furuyama A, Hirano S (2007) A murine scavenger receptor MARCO recognizes polystyrene nanoparticles. Toxicol Sci 97:398–406

Karin M, Cao Y, Greten FR, Li ZW (2002) NF-kappa B in cancer: from innocent bystander to major culprit. Nat Rev Cancer 2:301–310

Kasai H, Nishimura S (1984) Hydroxylation of deoxyguanosine at the C-8 position by ascorbic acid and other reducing agents. Nucleic Acids Res 12:2137–2145

Kobzik L (1995) Lung macrophage uptake of unopsonized environmental particulates. Role of scavenger-type receptors. J Immunol 155:367–376

Lam CW, James JT, McCluskey R, Hunter RL (2004) Pulmonary toxicity of single wall carbon nanotubes in mice 7 and 90 days after intratracheal instillation. Toxicol Sci 77:126–134

Lange SS, Takata K, Wood RD (2011) DNA polymerases and cancer. Nat Rev Cancer 11:96–110

Lindahl T, Wood RD (1999) Quality control by DNA repair. Science 286:1897–1905

Liu X, Lee J, Ji K, Takeda S, Choi K (2012) Potentials and mechanisms of genotoxicity of six pharmaceuticals frequently detected in fresh water environment. Toxicol Lett 211:70–76

Lobrich M, Shibata A, Beucher A, Fisher A, Ensminger M, Goodarzi AA, Barton O, Jeggo PA (2010) γH2AX foci analysis for monitoring DNA double-strand break repair. Strengths, limitations and optimization. Cell Cycle 9:662–669

Mantovani A, Allavena P, Sica A, Balkwill F (2008) Cancer-related inflammation. Nature 454:436–444

Matsumoto A, Naito M, Itakura H, Ikemoto S, Asaoka H, Hayakawa I, Kanamori H, Aburantani H, Tataku F, Suzuki H, Kobari Y, Miyai T, Takahashi K, Cohen EH, Wydro R, Houseman DE, Kodama T (1990) Human macrophage scavenger receptors: primary structure, expression and localization in atherosclerotic lesions. Proc Natl Acad Sci USA 87:9133–9137

Matsuzaki Y, Adachi N, Koyama H (2002) Vertebrate cells lacking FEN1 endonuclease are viable but hypersensitive to methylating agents and H_2O_2. Nucleic Acid Res 30:3273–3277

Monteiro-Riviere NA, Nemanich RJ, Inman AO, Wang YY, Riviere JE (2005) Multi-walled carbon nanotube interactions with human epidermal keratinocytes. Toxicol Lett 155:377–384

Muller J, Decordier I, Hoet PH, Lombaert N, Thomassen L, Huaux F, Lison D, Kirsch-Volders M (2008) Clastogenic and aneugenic effects of multi-wall carbon nanotubes in epithelial cells. Carcinogenesis 29:427–433

Murai J, Huang SY, Das BB, Renaud A, Zhang Y, Doroshow JH, Ji J, Takeda S, Pommier Y (2012) Trapping of PARP1 and PARP2 by clinical PARP inhibitors. Cancer Res 72:5588–5599

Murakumo Y, Roth T, Ishii H, Rasio D, Numata S, Croce CM, Fishel R (2000) A human REV7 homolog that interacts with the polymerase zeta catalytic subunit hREV3 and the spindle assembly checkpoint protein hMAD2. J Biol Chem 275:4391–4397

Nagai H, Okazaki Y, Chew SH, Misawa N, Yamashita Y, Akatsuka S, Ishihara T, Yamashita K, Yoshikawa Y, Yasui H, Jiang L, Ohara H, Takahashi T, Ichihara G, Kostarelos K, Miyata Y, Shinohara H, Toyokuni S (2011) Diameter and rigidity of multi-walled carbon nanotubes are critical factors in mesothelial injury and carcinogenesis. Proc Natl Acad Sci USA 108:1330–1338

Newman R, Schneider C, Sutherland R, Vodinelich L, Greaves M (1982) Trends Biochem Sci 7:397–400

Nojima K, Hochegger H, Saberi A, Fukushima T, Kikuchi K, Yoshimura M, Orelli BJ, Bishop DK, Hirano S, Ohzeki M, Ishiai M, Yamamoto K, Takata M, Arakawa H, Buerstedde JM, Yamazoe M, Kawamoto T, Araki K, Takahashi JA, Hashimoto N, Takeda S, Sonoda E (2005) Multiple repair pathways mediate tolerance to chemotherapeutic cross-linking agents in vertebrate cells. Cancer Res 65:11704–11711

Ock CY, Kim EH, Choi DJ, Lee HJ, Hahm KB, Chung MH (2012) 8-Hydroxydeoxyguanosine: not mere biomarker for oxidative stress, but remedy for oxidative stress-implicated gastrointestinal diseases. World J Gastroenterol 18:302–308

Ohmori H, Friedberg EC, Fuchs RP, Goodman MF, Hanaoka F, Hinkle D, Kunkel TA, Lawrence CW, Livneh Z, Nohmi T, Prakash L, Prakash S, Todo T, Walker GC, Wang Z, Woodgate R (2001) The Y-family of DNA polymerases. Mol Cell 8:7–8

Okada T, Sonoda E, Yoshimura M, Kawano Y, Saya H, Kohzaki M, Takeda S (2005) Multiple roles of vertebrate REV genes in DNA repair and recombination. Mol Cell Biol 25:6103–6111

Pacurari M, Yin XJ, Zhao J, Ding M, Leonard SS, Schwegler-Berry D, Ducatman BS, Sbarra D, Hoover MD, Castranova V, Vallyathan V (2008) Raw single-wall carbon nanotubes induce oxidative stress and activate MAPKs, AP-1, NF-kappa B, and Akt in normal and malignant human mesothelial cells. Environ Health Perspect 116:1211–1217

Palecanda A, Paulauskis J, Al-Mutairi E, Imrich A, Qin G, Suzuki H, Kodama T, Tryggvason K, Koziel H, Kobzik L (1999) Role of the scavenger receptor MARCO in alveolar macrophage binding of unopsonized environmental particles. J Exp Med 189:1497–1506

Polk DB, Peek RM Jr (2010) *Helicobacter pylori*: gastric cancer and beyond. Nat Rev Cancer 10:403–414

Rogakou EP, Boon C, Redon C, Bonner WM (1999) Megabase chromatin domains involved in DNA double-strand breaks in vivo. J Cell Biol 146:905–916

Shvedova AA, Castranova V, Kisin ER, Schwegler-Berry D, Murray AR, Gandelsman VZ, Maynard A, Baron P (2003) Exposure to carbon nanotube material: assessment of nanotube cytotoxicity using human keratinocyte cells. J Toxicol Environ Health A66:1909–1926

Shvedova AA, Kisin ER, Mercer R, Murray AR, Johnson VJ, Potapovich AI, Tyurina YY, Gorelik O, Arepalli S, Schwegler-Berry D, Hubbs AF, Antonini J, Evans DE, Ku BK, Ramsey D, Maynard A, Kagan VE, Castranova V, Baron P (2005) Unusual inflammatory and fibrogenic pulmonary responses to single-walled carbon nanotubes in mice. Am J Physiol Lung Cell Mol Physiol 289:L698–L708

Shvedova AA, Pietroiusti A, Fadeel B, Kagan VE (2012) Mechanisms of carbon nanotube-induced toxicity: focus on oxidative stress. Toxicol Appl Pharmacol 261:121–133

Sonoda E, Sasaki SM, Buerstedde JM, Bezzubova O, Shinohara A, Ogawa H, Takata M, Yamaguchi-Iwai Y, Takeda S (1998)

Rad51-deficient vertebrate cells accumulate chromosomal breaks prior to cell death. EMBO J 17:598–608

Sonoda E, Okada T, Zhao GY, Tateishi S, Araki K, Yamaizumi M, Yagi T, Verkaik NS, van Gent DC, Takata M, Takeda S (2003) Multiple roles of Rev3, the catalytic subunit of pol zeta in maintaining genome stability in vertebrates. EMBO J 22:3188–3197

Sutherland R, Delia D, Schneider C, Newman R, Kemshead J, Greaves M (1981) Ubiquitous cell-surface glycoprotein on tumor cells is proliferation-associated receptor for transferrin. Proc Natl Acad Sci USA 78:4515–4519

Takata M, Sasaki MS, Sonoda E, Morrison C, Hashimoto M, Utsumi H, Yamaguchi-Iwai Y, Shinohara A, Takeda S (1998) Homologous recombination and non-homologous end-joining pathways of DNA double-strand break repair have overlapping roles in the maintenance of chromosomal integrity in vertebrate cells. EMBO J 17:5497–5508

Takata M, Sasaki MS, Tachiiri S, Fukushima T, Sonoda E, Schild D, Thompson LH, Takeda S (2001) Chromosome instability and defective recombinational repair in knockout mutants of the five Rad51 paralogs. Mol Cell Biol 21:2858–2866

Thakur SA, Beamer CA, Migliaccio CT, Holian A (2009) Critical role of MARCO in crystalline silica-induced pulmonary inflammation. Toxicol Sci 108:462–471

Tomlinson CG, Atack JM, Chapados BR, Tainer JA, Grasby JA (2010) Substrate recognition and catalysis by flap endonucleases and related enzymes. Biochem Soc Trans 38:433–437

Van der Laan LJ, Dopp EA, Haworth R, Pikkarainen T, Kangas M, Elomaa O, Dijkstra CD, Gordon S, Tryggvason K, Kraal G (1999) Regulation and functional involvement of macrophage scavenger receptor MARCO in clearance of bacteria in vivo. J Immunol 162:939–947

Warheit DB, Laurence BR, Reed KL, Roach DH, Reynolds GA, Webb TR (2004) Comparative pulmonary toxicity assessment of single-wall carbon nanotubes in rats. Toxicol Sci 77:117–125

Wick P, Manser P, Limbach LK, Dettlaff-Weglikowska U, Krumeich F, Roth S, Stark WJ, Bruinink A (2007) The degree and kind of agglomeration affect carbon nanotube cytotoxicity. Toxicol Lett 168:121–131

Wu X, Takenaka K, Sonoda E, Hochegger H, Kawanishi S, Kawamoto T, Takeda S, Yamazoe M (2006) Critical roles for polymerase zeta in cellular tolerance to nitric oxide-induced DNA damage. Cancer Res 66:748–754

Yamazoe M, Sonoda E, Hochegger H, Takeda S (2004) Reverse genetic studies of the DNA damage response in the chicken B lymphocyte line DT40. DNA Repair 3:1175–1185

Ye SF, Wu YH, Hou ZQ, Zhang QQ (2009) ROS and NF-kappa B are involved in upregulation of IL-8 in A549 cells exposed to multi-walled carbon nanotubes. Biochem Biophys Res Commun 379:643–648

Yoshimura M, Kohzaki M, Nakamura J, Asagoshi K, Sonoda E, Hou E, Prasad R, Wilson SH, Tano K, Yasui A, Lan L, Seki M, Wood RD, Arakawa H, Buerstedde JM, Hochegger H, Okada T, Hiraoka M, Takeda S (2006) Vertebrate POLQ and POLbeta cooperate in base excision repair of oxidative DNA damage. Mol Cell 24:115–125